

Review

Review of Electrochemical Testing to Assess Corrosion of Post-Tensioned Tendons with Segregated Grout

Samanbar Permeh * and Kingsley Lau

Department of Civil and Environmental Engineering, Florida International University, Miami, FL 33174, USA; kilau@fiu.edu

* Correspondence: samanbar.permeh1@fiu.edu

Abstract: Post-tensioned (PT) construction incorporating bonded tendons with cementitious grouts has been used for highway bridges. The tendon duct and the encapsulating grout materials provide barrier corrosion protection for the embedded high-strength steel strand. Although generally used in good engineering practice, cases of PT tendon corrosion have been documented relating to inadequate detailing for joints and development of grout bleed water. Recently, in the past several years, unexpected severe localized strand corrosion has related to the segregation of thixotropic grouts. In the latter case, thixotropic grouts (that have been developed to mitigate grout bleeding) formed physical and chemical deficiencies that have been characterized to have high moisture content and elevated sulfate ion concentrations. The early presence of elevated sulfate ion concentrations in the deficient grout hinders stable steel passivation. The corrosion mechanism can be complicated due to the compounding effects of physical grout deficiency, moisture content, pore water pH, and the presence of sulfate ions. There remains interest to reliably assess corrosion of PT tendons with deficient grout. A review of electrochemical techniques and test methods used in earlier research by the authors to identify the role of sulfates on localized steel corrosion in alkaline solutions is presented. It was evident that different testing methods can reveal various aspects of the corrosion of strands in the deficient PT grout. The open-circuit potential and linear polarization method could differentiate corrosion activity between hardened and deficient grout environments but did not reveal the development of localized corrosion. Electrochemical impedance spectroscopy was useful to identify grout deficiencies by the differentiation of its bulk electrical properties. Potentiodynamic polarization and electrochemical noise technique were used to identify metastable and pitting in alkaline sulfate solutions representative of the deficient grout pore water.

Keywords: post-tensioned (PT); grout; corrosion; electrochemical; testing



Citation: Permeh, S.; Lau, K. Review of Electrochemical Testing to Assess Corrosion of Post-Tensioned Tendons with Segregated Grout. *Constr. Mater.* **2022**, *2*, 70–84. <https://doi.org/10.3390/constrmater2020006>

Received: 14 February 2022

Accepted: 28 March 2022

Published: 8 April 2022

Publisher's Note: MDPI stays neutral with regard to jurisdictional claims in published maps and institutional affiliations.



Copyright: © 2022 by the authors. Licensee MDPI, Basel, Switzerland. This article is an open access article distributed under the terms and conditions of the Creative Commons Attribution (CC BY) license (<https://creativecommons.org/licenses/by/4.0/>).

1. Introduction

Post-tensioning (PT) systems have been widely used for bridge construction since the late twentieth century due to the opportunity for greater design choices available by construction technology [1]. The prestressing afforded by the PT provides reinforcement to the concrete structural element to minimize deflection and cracking, and PT systems can be utilized to construct efficient bridge structures with longer clear spans. Bonded PT systems incorporate tendons comprising prestressed high-strength steel strand/rod encapsulated within a plastic or galvanized steel duct by a cementitious grout. Bonded tendons have several advantages for the strength and service of the bridge. In addition to mechanical benefits such as the development of forces along the length of the tendon, the encapsulating grout provides corrosion protection of the steel by serving as an additional physical barrier to the environment and external contaminants as well as allowing the development of a protective passive oxide film on the steel due to the high grout pore water pH. Even though the technology has ideally excellent durability traits, complexities of design details,

construction, material specification and application, and sometimes non-conformity to good practice have led to several cases of corrosion of the prestressing steel [2].

Corrosion of PT tendons has been documented since the late 1960s and up to recent times. From the late 1990s, corrosion of external tendons in Florida and Virginia bridges was accounted by the accumulation of grout bleed water and subsequent formation of grout voids [3–6]. The events in the 1990s spurred the development and specification of high-performance cementitious grouts in the early 2000s to minimize bleed water formation. After that time, pre-packaged thixotropic grout materials were specified to improve onsite construction quality. In the past 10 years, there were a few PT bridges nationwide where the high-performance grout exhibited physical deficiencies characterized by high moisture content, high pH, and elevated concentrations of alkali and sulfate ions [7–9]. The deficient grout (Figure 1) was directly associated with significant corrosion of strand or steel PT components in 2 bridges in Florida [10–14] and coincided with strand and duct corrosion in 2 bridges in Virginia. In 2011, corrosion failures of external tendons in a post-tensioned segmental box bridge (built-in 2003) in Florida occurred [7]; and shortly after, severe corrosion of galvanized steel internal tendon ducts in another Florida bridge (built-in 2004) was detected. The response included research to assess the corrosion risk of steel in grouts with elevated chloride ion concentrations, elevated free sulfate concentrations, and provided guidelines for sampling and testing [15–23]. Lee, 2021 reevaluated the influence of elevated sulfate ion concentrations in deficient grout by anodic potentiodynamic polarization test and suggested that sulfates can be aggressive at depressed pore water pH [17].

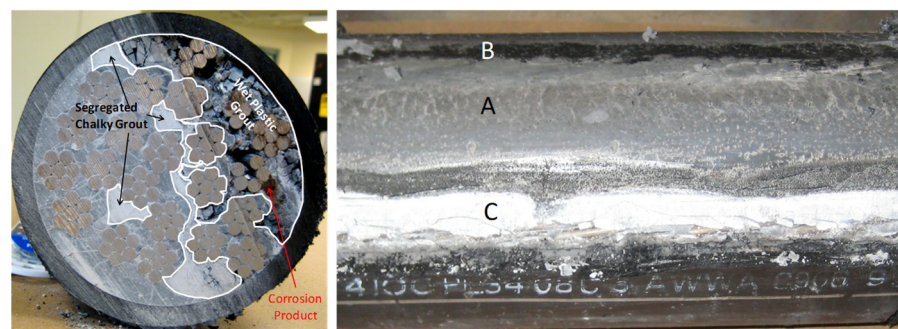


Figure 1. Grout segregation. A. Wet plastic grout. B. Band of silica fume. C. White chalky grout [8].

Other recent research relating to corrosion of strand in deficient grout involved non-destructive testing [24–26] and imaging techniques [27,28] to identify physical grout deficiencies (using impedance spectroscopy, magnetic flux leakage, and main magnetic flux method), numerical modeling to project service [29,30], and remediation with inhibitor impregnation [31,32]. Hamilton et al., 2014 [33] addressed the development of deficient grout in tendons by a modified version of the inclined tube test where temperature, humidity, and excess water content tested to identify the propensity for segregation. Hamilton et al., 2018 [34] further identified that adverse effect of prolonged exposure of the grout to humidity and recommended control of product shelf-life and packaging. Hamilton et al., 2020 [35] evaluated removal and repair of tendons containing segregated grout by hydro-demolition and tendon drying and identified challenges associated with entrapped water and grout carbonation. Whitmore et al., 2020 [36] developed an inhibitor impregnation system demonstrating that a protective film can be introduced through the strand interstitial spaces and can reduce corrosion. Rehmat et al., 2019 [37] discussed the use of the magnetic main flux method and ultrasonic testing to identify strand cross-section loss and grout anomalies in tendons containing segregated grout. A novel indirect impedance technique and magnetic imaging technique were developed by Alexander et al., 2017 [24] and Dukeman et al., 2019 [28]; respectively. Conventional NDTs were reviewed by Azizinamini et al., 2012 [27] and Hurlebaus et al., 2018 [38]. The reviews indicated that technologies to detect segregated grout are available.

The steel strand corrosion associated with segregated grout was observed to be localized to regions where the grout developed physical and chemical deficiencies [13]. The grout in well-hydrated condition typically had a moisture content of 20%. The localized deficient grout had greater moisture content that exceeded 60% and sometimes as high as 80%. As shown in Figure 2, that deficient grout also had elevated concentrations of sulfates (>10,000 ppm) and alkalis (potassium and sodium). The grout pore water pH of the deficient grout was generally found to be similar to that of non-carbonated grouts and typically exceeded 12 with some exception for grouts adjoining anodic steel regions where severe corrosion had already developed. Analysis of electrochemical testing was challenging due to the discrepant understanding of the role of sulfate ions in alkaline solutions. A more thorough review of the literature is found in references [8,39]. The literature generally concedes that elevated sulfate concentrations in less alkaline pore solutions were found to have an adverse effect on the stability of the passive film but corrosion behavior in test solutions differ in otherwise chemically similar cementitious materials. Autocatalytic corrosion with local acidification can develop within corrosion pits similar to that for chlorides as described by Equation (1) [40].

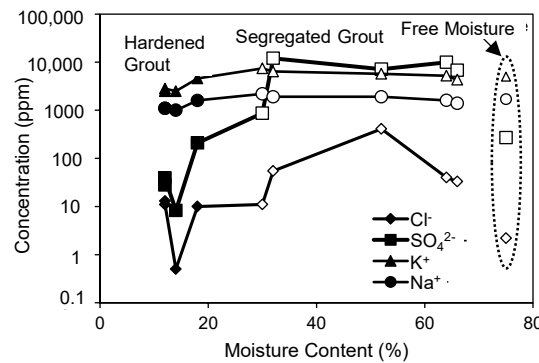
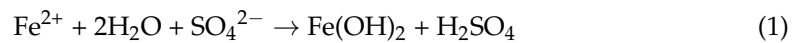


Figure 2. Ionic constituents in grout leachate [8]. Black. Hardened grout. White. Segregated grout.

The corrosion mechanism can be complicated due to the compounding effects of the physical grout deficiency, moisture content, pore water pH, and the presence of sulfate ions. Indeed, discrepant research findings have been presented in the literature in part due to complications and limitations in the electrochemical techniques. For example, the onset of localized corrosion may not be well captured by conventional open-circuit and linear polarization resistance measurements often used by practitioners. There remains interest in the corrosion assessment of PT tendons with deficient grout to identify corrosion activity, corrosion rates, and grout conditions in both field and laboratory testing. A review of electrochemical techniques and test methods used in earlier research by the authors to identify the role of sulfates on localized steel corrosion in deficient grout materials and representative alkaline sulfate solutions is presented. Examples of the outcomes of electrochemical testing on the role of sulfate ions are described next in the spirit to provide the readers a general view of how the presented test methods can be applied to assess the negative effects of chemically and physically deficient grout on PT corrosion.

2. Open-Circuit Potential

The open-circuit potential (OCP) or corrosion potential (E_{corr}) is a common electrochemical parameter used for corrosion assessment of reinforced concrete bridge elements [41,42]. The OCP delineates the steady-state condition of the electrochemical reactions where the sum of all anodic reactions, such as iron oxidation, is equal to the sum of all cathodic reactions including oxygen reduction. Steel in alkaline pore water solutions ideally would develop passivity where the rate of the anodic reaction would be relatively constant at a low passive corrosion rate regardless of the amount of anodic overvoltage from the equilibrium condition that develops by the coupling to the reduction reactions. More electronegative OCP such as that defined in ASTM C876 [43] would develop if active corrosion develops causing the anodic branch of the polarization curve to develop a smaller anodic Tafel slope. Thus, the measurement can give a quick assessment of passive or active corrosion conditions assuming concentration polarization of the reduction reactions is not dominant. The measurement requires an electrical connection to the reinforcing/prestressing steel and ionic contact to the surface of the cementitious material. In situ measurements of PT tendons would require a partial opening of the duct. The surface of the steel element serves as the working electrode connected to a high input-impedance voltmeter. An external reference electrode such as a copper/copper-sulfate reference electrode (CSE) is rastered on the element surface along the length of the steel and adjoining electrically continuous steel to provide a surface map of potentials that can indicate corrosion activity. For reinforced concrete, ASTM C876 lists value criteria for corrosion potential. OCP more electronegative than $-0.35 \text{ V}_{\text{CSE}}$ is generally considered as a marker for active corrosion [43].

Bridge tendon sections containing partial filling with deficient grout (in soft and chalky form) and hardened grout, as shown in Figure 1, containing varying sulfate ion concentrations (in the order of 10–100 ppm in hardened grout and 1000 to 10,000 in deficient grout) resulted in a distribution of OCP such as shown in Figure 3. Steel strands embedded in the well-hardened grout typically developed more electropositive potentials indicative of passive conditions, whereas steel strands adjacent to the deficient grout developed more electronegative potentials. Similarly, differentiation in corrosion potentials developed in steel corrosion probes installed in a modified incline-tube (MIT) test, where the active corrosion potentials developed at higher elevations (where grout segregation was induced), and passive corrosion potentials developed at lower elevations [8,39,44–46]. As shown in Figure 4, electronegative potentials developed in alkaline solutions with elevated sulfate concentrations.

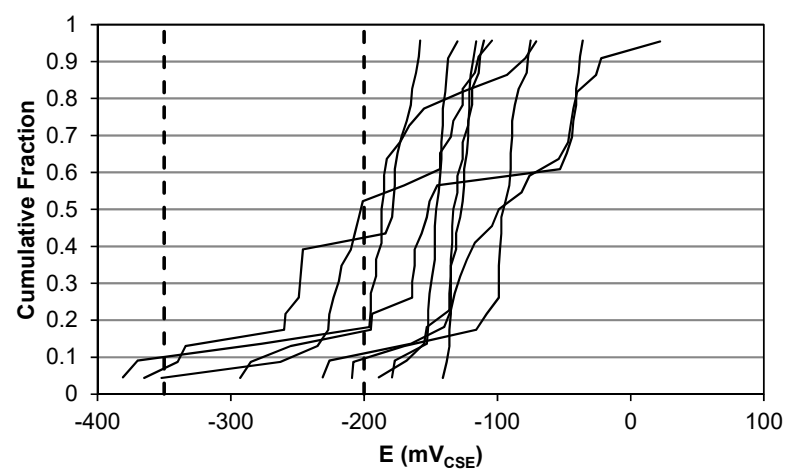


Figure 3. Distribution of steel strand OCP from a PT tendon partially filled with deficient grout [8]. Vertical lines represent guidelines for corrosion activity defined by ASTM C876.

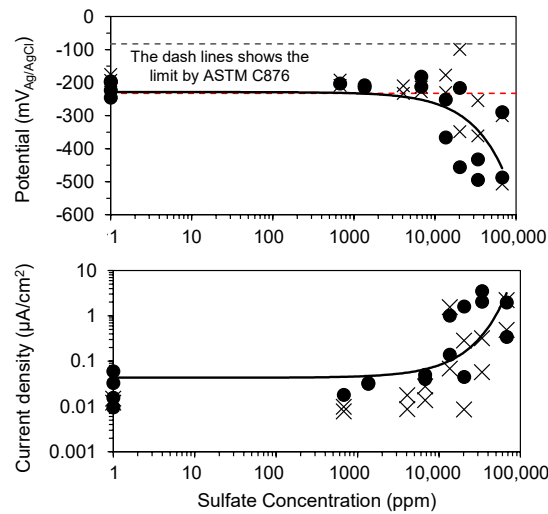


Figure 4. Corrosion potential and corrosion rates of steel in alkaline sulfate solutions [39]. Black circle indicate data after 24 h of testing and crosses measured after 1 week of immersion in solution.

3. Linear Polarization Resistance

The linear polarization resistance (LPR) measurement allows for the assessment of corrosion rates [40,47]. Like OCP measurements, electrical contact to the steel working electrode and ionic contact of a reference electrode (such as a CSE) to the element surface is required. A counter electrode with ionic contact to the element surface is also required as part of the three-electrode configuration. A potentiostat is used to provide current via the counter electrode to induce a small amount of polarization near the OCP measured between the working and reference electrode. The ratio of the change in the potential to the change in current density (compensated for solution resistance, R_s) is defined as the polarization resistance, R_p [48].

$$R_p = \frac{dE}{di} - R_s \tag{2}$$

The corrosion current density i_{corr} can be estimated by the relationship $i_{corr} = B/R_p$ where the Stern-Geary coefficient, B , associated with the anodic and cathodic Tafel slope is often assumed to be 26 mV for active uniform corrosion conditions and 52 mV for passive conditions [40]. Potentiodynamic polarization tests for steel in alkaline sulfate solutions by Vigneshwaran et al., 2018 [49] showed B values for active and passive conditions in the order of 16–21 and 24–55 mV, respectively

Field measurements can be complicated due to geometric constraints to setup the test electrodes. Furthermore, complications with current attenuation exist and application of guard-ring counter electrodes have been made for reinforced concrete elements. Nevertheless, LPR measurements have been useful to identify corrosion activity related to grout segregation.

Results by Permeh et al., 2018 [46], from LPR testing of steel corrosion probes installed along the length of the 15-foot tendon mockup test specimens inclined at 30 degrees in MIT testing showed strong differentiation in steel corrosion rates between the upper elevations of the inclined tube from those at lower elevations. The MIT tests allowed for some level of grout deficiencies to form at the top elevations resulting in corrosion current densities approximately one order of magnitude greater than that estimated for steel in the hardened grout at lower elevations (Figure 5). The OCP for the corrosion probes embedded in the upper tendon elevation were generally more electronegative than -300 mV_{CSE} and $\sim -220 \text{ mV}_{CSE}$ in the hardened grout at lower elevations. Nominal i_{corr} values were in the order of $0.1 \text{ } \mu\text{A}/\text{cm}^2$ to $0.01 \text{ } \mu\text{A}/\text{cm}^2$ for steel in segregated and hardened grout, respectively. Corrosion rates estimated by LPR for steel in alkaline sulfate solutions are shown in Figure 4. The corrosion rates showed a good correlation to the sulfate concentration; however, local corrosion pits developed in some of those steel test

specimens that had modest calculated corrosion rates. Both OCP and LPR measurements can provide differentiation between active and passive corrosion conditions of steel strand embedded in grout but may not necessarily elucidate localized corrosion activity observed in metastable and stable pitting associated with the elevated sulfate ion concentrations.

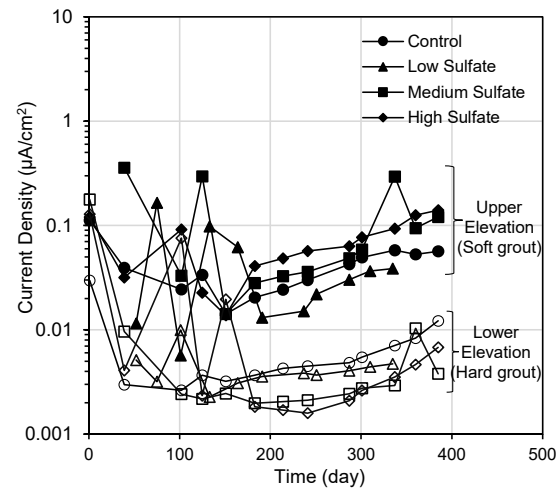


Figure 5. Corrosion rates of probes in MIT tests estimated by LPR [46]. Black. Upper elevations (Deficient grout). White. Lower elevations (Hardened grout).

4. Macrocell Corrosion

Macrocell corrosion develops due to the adverse galvanic coupling of steel electrodes with differential corrosion conditions. The active corrosion rate of steel in regions where passivity is lost can be elevated when that steel is coupled to extended cathodes elsewhere that can support a greater level of reduction reactions, including oxygen reduction. The PT tendons that had corrosion failures associated with segregated grout had localized regions of deficient grout along the length of the tendon, as well as within the cross-section, as shown in Figure 1. It was visually evident from the tendon failure that the corrosion coincided with the deficient grout. The fast corrosion was thought to be exacerbated by macrocell coupling of localized anodic regions embedded in the deficient grout and extended cathodes on the steel strand along the length of the tendon throughout. As described earlier, the OCP of the steel in the deficient grout was more electronegative than that in the hardened grout. Coupling of these electrodes would cause some level of anodic polarization of the anodic regions, supported by oxygen reduction reactions throughout the tendon, and accelerate the corrosion rate of the steel in the deficient grout.

Macrocell corrosion testing consists of ionically and electrically coupling two cell components. One of the cells has net anodic behavior and the other has net cathodic behavior. Several test setups relating to grout materials have been described in the literature and can include using salt bridges to ionically couple separate electrolytes [50–53]. Current between the two electrically coupled electrodes can be made via shunt resistors and electrical switches. Macrocell corrosion testing relating to the segregated grout was made by coupling separate cut bridge tendon sections, one of which contained deficient grout and the other with only hardened grout. As shown in Figure 6, coupling of the tendon sections allowed for the development of an intermediate cell potential more electropositive than the OCP of the strand in the section with segregated grout [8,12,54]. This provided an anodic polarization that exceeded 50 mV and provided a net anodic macrocell current.

Recent research applied macrocell corrosion to develop practical test methods to assess the robustness of grout materials to corrosion cast with non-ideal construction practices [55–58].

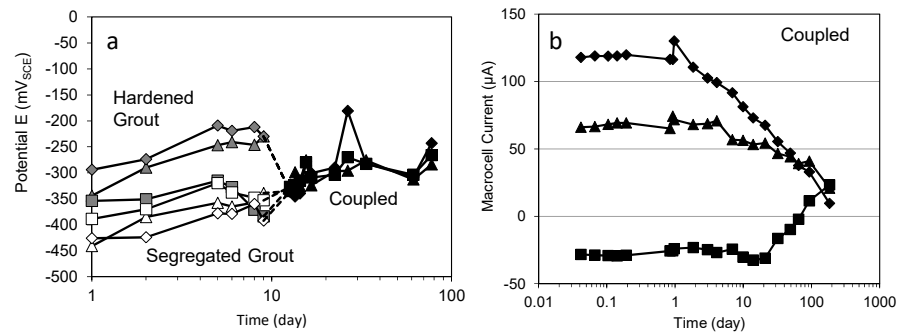


Figure 6. Macrocell coupling of tendon sections with segregated and hardened grout [12]. (a) Coupled potential. (b) Macrocell current. Positive macrocell currents represent net anodic current.

5. Anodic Potentiodynamic Polarization

Anodic potentiodynamic polarization scans provide information on the anodic behavior of metals in solution [40]. These measurements have been useful for the assessment of corrosion-resistant alloys and the identification of localized corrosion. The elevated sulfate ion concentrations in the deficient grout coincided with severe localized corrosion and was thought to have an adverse effect on the stability of the passive film. Anodic potentiodynamic polarization scans were made for grouted steel specimens as well as in alkaline sulfate solutions in the laboratory to elucidate the anodic behavior of steel in deficient grout with enhanced sulfate ion levels and determine if more adverse corrosion conditions exist in deficient grout [17,59,60]. Details can be found in [49,61,62].

Anodic polarization scans made for steel probes in the MIT testing (Figure 7) generally showed passive-like characteristics for all test cases, including in specimens with sodium sulfate admixed in the grout [46] although more electronegative OCP developed in the cases with admixed sodium sulfate. With the highest level of externally admixed sulfate, a feature of the polarization graph showed an abrupt increase in anodic current for steel in the upper portions of the tendon.

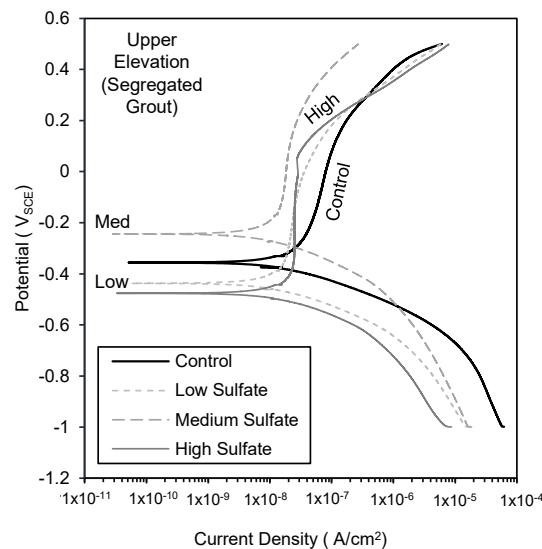


Figure 7. Anodic potentiodynamic polarization scan of steel in PT grout [46].

Testing in alkaline sulfate solutions yielded better differentiation in corrosion behavior. Results by Krishna Vigneshwaran et al., 2018 [59] indicated that the early presence of pre-mixed sulfate ions in saturated calcium hydroxide solution (pH ~ 12.6) could be aggressive by impairing the initial passive film development. As shown in Figure 8, higher passive-like corrosion current densities developed in the presence of sulfate ions indicating an increase in the anodic current exchange density. Active corrosion characteristics developed

above 16,000 ppm Na_2SO_4 . Permech et al., 2021 [39], used cyclic anodic potentiodynamic polarization scans made from the OCP to values as high as 400 mV_{Ag/AgCl} with a forward scan rate of 0.01 mV/s and a reverse scan rate of 0.1 mV/s. Large anodic Tafel slopes were generally observed. The anodic current densities increased and the OCP dropped to more electronegative values with higher sulfate concentrations. The more electronegative OCP at higher sulfate concentrations may be related to the increase in the anodic current exchange density and complicates the conventional interpretation of corrosion potentials by practitioners such as in ASTM C876 relating to passive to active corrosion transitions. Below 20,000 ppm Na_2SO_4 , the reverse scan showed a negative hysteresis indicating passive corrosion conditions, but the onset of metastable pitting (>2000 ppm Na_2SO_4) was observed by the transient current excursions that developed during the polarization. Above 20,000 ppm Na_2SO_4 , the polarization scans showed a positive hysteresis curve as well as pitting events characterized by the sharp increase in corrosion current.

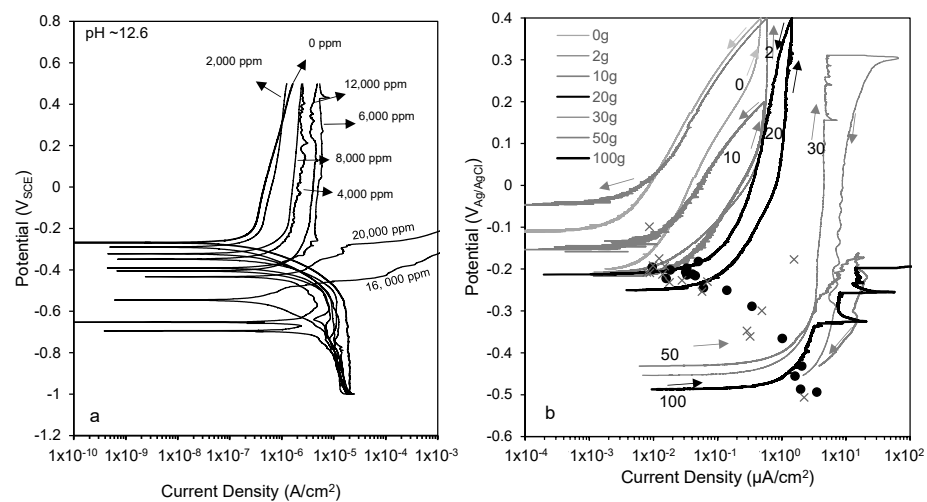


Figure 8. Anodic potentiodynamic polarization of steel in an alkaline sulfate solution. (a) Potentiodynamic polarization in pH 12.6 sulfate solution [49]. (b) Cyclic Polarization in pH 12.6 sulfate solution (values in legend correspond to g Na_2SO_4 per L H_2O) [39].

6. Electrochemical Impedance Spectroscopy

Electrochemical impedance spectroscopy (EIS) encompasses several techniques, among which the potentiostatic method at the OCP (i.e., no applied DC voltage bias) allows for corrosion assessment of metals in an electrolyte. The technique not only characterizes interfacial characteristics, such as polarization resistance, but also provides information on bulk solution characteristics, surface characteristics, transport characteristics, and current distribution [63,64]. These benefits can parse system components that can cause an error in testing (such as LPR) but can also convolute practical assessment of complicated systems. Like LPR and other polarization methods, EIS also utilizes the three-electrode system. Unlike the DC methods, EIS applies an AC potential polarization at various frequencies from which the current is measured, and the impedance time constants associated with various system parameters can be gaged. EIS is often analyzed utilizing equivalent circuit analogs to which the impedance of the bulk, interfacial, and transport parameters can be mathematically characterized to corollary electrical components. Similar practical constraints for LPR testing in bridge systems apply for EIS. Pertinent system parameters relevant to the corrosion of strands in segregated grout include the charge-transfer resistance (R_{ct}) relating to the corrosion rate and the solution resistance (R_s) which can gage the quality of the bulk grout material. The Randles circuit has been widely considered to assess the interfacial parameters (double-layer capacitance, C_{dl} , and charge-transfer resistance, R_{ct}) of corrosion

systems (Equation (3)), but advanced treatments to account for intermediate layers, surface heterogeneities, and other system parameters have been developed.

$$Z = R_s + \frac{1}{j\omega Cdl + \frac{1}{R_{ct}}} \tag{3}$$

Lau et al., 2012 [65] provided preliminary results on the application of EIS to characterize grout properties and corrosion conditions of the strand. Recovered tendon sections from the failed PT tendon were used to fabricate test specimens. Potentiostatic EIS measurements at OCP were made with a frequency range $100 \text{ kHz} > f > 1 \text{ mHz}$ with an A.C. rms amplitude of 10 mV. The analysis generally assumed that the high-frequency limit of the impedance spectra corresponded to the solution resistance of the grout material and the low-frequency limit corresponded to the metal-solution interface properties. The technique was sensitive to the degree of moisture and hydration of cementitious material as well as the general corrosion condition of the embedded steel. The presence of a high-frequency loop in the impedance spectra in Nyquist form (Figure 9) was suggested to be related to the dielectric response of the different cementitious materials present in the system with possible application to characterize tendons with dissimilar grouts. Consistent with the observed grout segregation, that component of the impedance response was significantly lower than that of the tendon samples from locations without major grout segregation. As shown in Figure 10, solution resistance of grout in MIT testing [46] shows differentiation between the grout in the upper elevation segregated grout and lower elevation hardened grout.

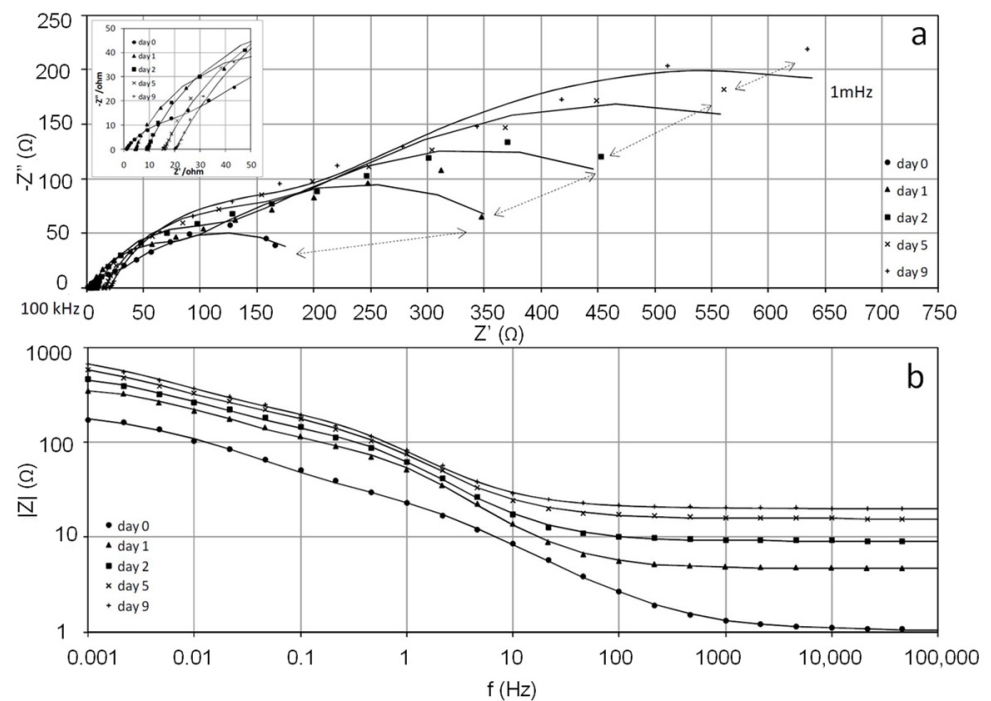


Figure 9. Example of impedance results of steel strand in grouted PT tendon, (a) Nyquist plot, (b) Bode plot [65].

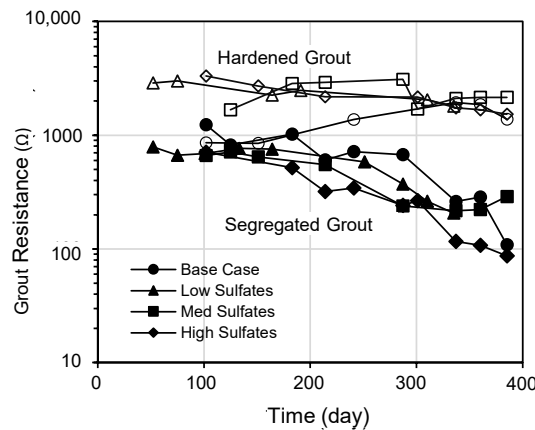


Figure 10. Example of grout solution resistance from MIT testing [46]. Black: Segregated grout. White: Hardened grout.

7. Electrochemical Noise

Testing of steel in alkaline sulfate solutions showed that localized corrosion can develop. OCP, LPR, macrocell, and EIS testing does not necessarily clarify this corrosion modality. The anodic potentiodynamic polarization test elucidates pitting corrosion development and provides an indication of metastable pitting by the transient current fluctuations. The electrochemical noise (EN) technique assesses ambient electrochemical fluctuations at the steel surface that develop due to local disruptions of the passive film and local active corrosion events. EN ideally could elucidate the localized corrosion behavior of steel subjected to the early presence of elevated sulfate ion concentrations in alkaline solutions. Examples of EN events for steel in alkaline sulfate solutions are shown in Figure 11.

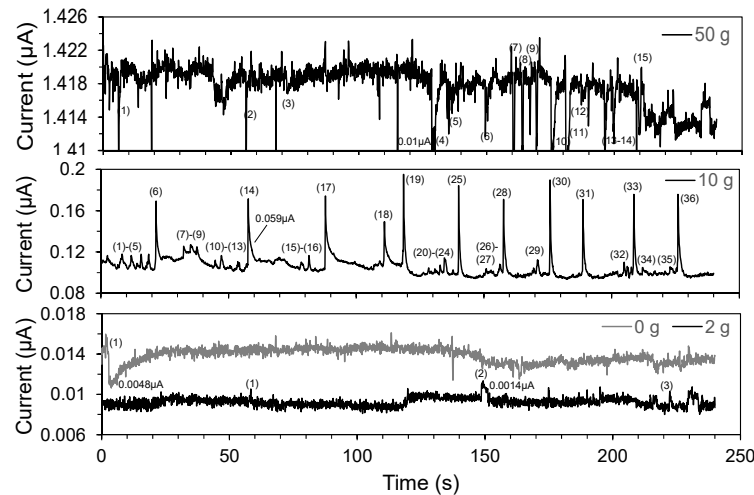


Figure 11. Example of EN current events in alkaline sulfate solutions [33].

EN measurements have evolved over the years and several test setup configurations have been implemented. A comprehensive review is provided in refs. [39,66,67]. Generally, EN test setup requires two nominally identical steel electrodes connected across a zero-resistance ammeter (ZRA) with a stable reference electrode. Appropriate anti-aliasing filters and instrument settings are required [68,69]. The EN data can be analyzed in the time domain by statistical evaluation of the electrochemical potential and current time signatures such as the mean, rms, standard deviation, skew, and kurtosis. Deviations from a normal distribution can be inferred from the spontaneous events associated with the local disruption of the passive film. The spectral analysis includes assessment of the power spectral density (PSD), as shown in Figure 12, to characterize the characteristic

charge (q), characteristic frequency (f_n), and corrosion current, (I_{corr}). Additionally, comparisons of the noise impedance (Z_n) and noise resistance (R_n) can be made. The noise resistance ($Rn = \sigma_E / \sigma_I$) has often been compared with the polarization resistance.

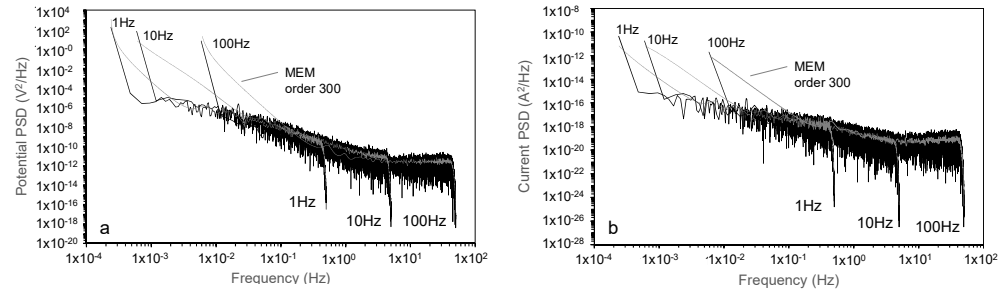


Figure 12. Example of (a) potential and (b) current PSD by FFT and MEM [46].

Characteristics of the transient events can be assessed from the PSD by shot noise analysis. The PSD would ideally show a low-frequency limit (Ψ_{E0} for potential and Ψ_{I0} for current) but assuming a nominal Ψ_{E0} and Ψ_{I0} at a low frequency such as at 1 mHz can provide adequate qualitative comparisons of the noise parameters. The corrosion current was described as

$$I_{corr} = B \sqrt{\frac{\Psi_{I0}}{\Psi_{E0}}} \tag{4}$$

where B is the Stern–Geary coefficient and is related to the noise admittance $Z_n^{-1} = (\Psi_{I0}/\Psi_{E0})^{0.5}$. The characteristic charge, q , of the transient events was described as

$$q = \frac{\sqrt{\Psi_{I0} \times \Psi_{E0}}}{B} \tag{5}$$

and the characteristic frequency, f_n , of the transient events was described as

$$f_n = \frac{B^2}{\Psi_{E0}} \tag{6}$$

Results of EN testing of steel in alkaline sulfate solution by [39] are shown in Figure 13. The general trend indicated that the characteristic charge increases and the characteristic frequency decreases with sulfate ion concentration, yet the overall corrosion rate increases. This would consist of more extensive localized corrosion at higher sulfate concentrations.

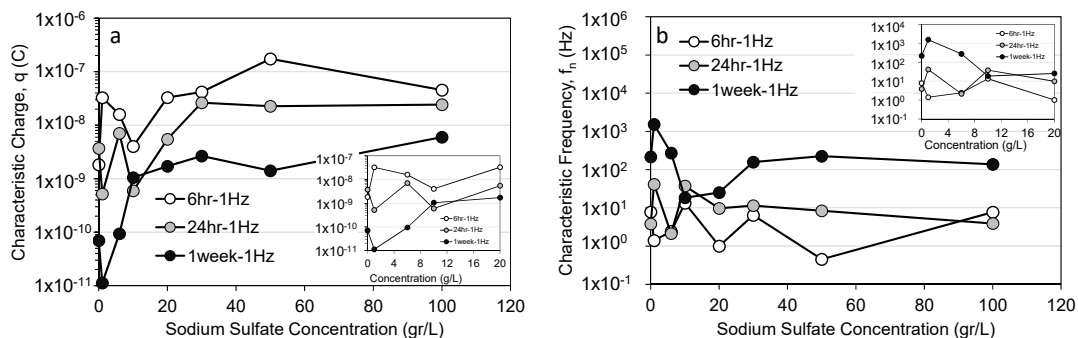


Figure 13. EN (a) characteristic charge, q and (b) frequency, f_n in sulfate solutions [39].

8. Overview of Steel Strand Corrosion in Deficient Grout

It was evident that the severe and highly localized corrosion of the steel strand was associated with the deficient grout coincident with elevated sulfate concentrations. Through a series of research utilizing various electrochemical testing techniques as reviewed in the preceding, the corrosion behavior of steel strands in deficient grout can be clarified. The

relatively high pH > 12, low-level chloride content, and inconsistent coincidence of grout voids indicated that the conventional means of chloride-induced or carbonation-induced corrosion were not the dominant mechanisms for the failure. The electrochemical testing of field-extracted and lab test specimens revealed that elevated concentrations of sulfate ions in moderately alkaline pH solutions (i.e., pH ~ 12.6) can allow the destabilization of the passive film where initially localized metastable and stable pitting can occur. Testing in solution indicated that local disruption of the passive film can develop above 2000 ppm Na₂SO₄ and local corrosion can develop above 20,000 ppm Na₂SO₄. However, the passive film stability is largely influenced by the pH. Testing in sulfate solutions at pH > 13 did not develop corrosion [49] and pH > 14 can allow for active steel dissolution [59]. The critical concentration values in relation to pH require clarification [19]. Once local disruption to the passive film develops, macrocell coupling of the local anode to the rest of the strand assembly can allow adverse galvanic coupling and anodic polarization that would promote pitting.

Assessment of the effect of the deficient grout with its lower binder content on sulfate and chloride ion binding is warranted as is the synergistic effect of sulfate ions and low-level chloride ions on steel depassivation. Initial research on these topics is discussed in [19]. The development of practical sulfate limits for grout materials and testing for material robustness is discussed in [56,57].

9. Conclusions

Assessment of the corrosion mechanism of steel strands in segregated grout with elevated sulfate concentrations has been difficult due to discrepant information on the role of sulfates on corrosion initiation in the literature. Electrochemical testing would ideally elucidate the role of the sulfates. Corrosion potentials and current densities (OCP and LPR testing) are good indicators of active corrosion for steel in elevated sulfate environments (differentiating behavior of steel in hardened and deficient grouts) and support the supposition that macrocell coupling (macrocell corrosion) of strands in the deficient grout with the rest of the strand within the tendon allows for aggravated corrosion conditions. However, these techniques would not necessarily capture the propensity for pitting. Anodic potentiodynamic polarization testing revealed that the anodic current exchange densities can increase at high sulfate concentrations and account for the manifestation of more electronegative OCP and higher corrosion rates. Metastable pitting and pitting were characterized by anodic current excursions at the elevated sulfate concentrations. Electrochemical noise (EN) testing revealed the metastable and stable pitting events that can occur in alkaline sulfate solutions. Electrochemical impedance spectroscopy (EIS) can identify corrosion rates and, importantly, characteristics of the bulk grout material that can differentiate hardened and deficient grouts.

Author Contributions: Writing-Review and Editing, S.P. and K.L. All authors have read and agreed to the published version of the manuscript.

Funding: This research received no external funding.

Data Availability Statement: All data contained within the article.

Conflicts of Interest: The authors declare no conflict of interest.

References

1. Hewson, N.R. *Prestressed Concrete Bridges: Design and Construction*; Thomas Telford Publishing: London, UK, 2003.
2. Lau, K.; Lasa, I. Corrosion of prestress and post-tension reinforced-concrete bridges. In *Corrosion of Steel in Concrete Structures*; Poursaei, A., Ed.; Woodhead Publishing: Cambridge, UK, 2016; pp. 37–57. [[CrossRef](#)]
3. Powers, R.G. *Corrosion Evaluation of Post-Tensioned Tendons on the Niles Channel Bridge*; Florida Department of Transportation: Tallahassee, FL, USA, 1999.
4. Corven Engineering. *Mid-Bay Bridge Post-Tensioning Evaluation*; Final Report to Florida Department of Transportation; The Florida Department of Transportation Research Center: Tallahassee, FL, USA, 10 October 2001.

5. Hartt, W.; Venugopalan, S. *Corrosion Evaluation of Post-Tensioned Tendons on the Mid Bay Bridge in Destin, Florida*; Final Report to Florida Department of Transportation; Florida Department of Environmental Protection: Tallahassee, FL, USA, April 2002.
6. Hansen, B. Forensic Engineering: Tendon Failure Raises Questions about Grout in Post-Tensioned Bridges. *Civ. Eng. News* **2007**, *77*, 17–18.
7. Lau, K.; Lasa, I.; Paredes, M. *Corrosion Development of PT Tendons with Deficient Grout: Corrosion Failure in Ringling Causeway Bridge*; Draft Report; Florida Department of Transportation State Materials Office: Gainesville, FL, USA, 2011.
8. Permeh, S.; Krishna Vigneshwaran, K.K.; Lau, K. *Corrosion of Post-Tensioned Tendons with Deficient Grout*; Final Report to Florida Department of Transportation, Contract No. BDV29-977-04; Florida Department of Transportation: Tallahassee, FL, USA, 20 October 2016.
9. Sprinkel, M.M.; Balakumaran, S.S.G. Problems with Continuous Spliced Posttensioned–Prestressed Concrete Bulb-Tee Girder Center Spans at West Point, Virginia. *Transp. Res. Rec.* **2017**, *2642*, 46–54. [[CrossRef](#)]
10. Lau, K.; Powers, R.; Paredes, M. Corrosion Evaluation of Repair-Grouted Post-Tensioned Tendons in Presence of Bleed Water. In Proceedings of the CORROSION 2013, Orlando, FL, USA, 17–21 March 2013; NACE International: Houston, TX, USA, 2013.
11. Lau, K.; Rafols, J.; Paredes, M.; Lasa, I. Laboratory Corrosion Assessment of Post-Tensioned Tendons Repaired with Dissimilar Grout. In Proceedings of the CORROSION 2013, Orlando, FL, USA, 17–21 March 2013; NACE International: Houston, TX, USA, 2013.
12. Lau, K.; Paredes, M.; Lasa, I. Corrosion Failure of Post-Tensioned Tendons in Presence of Deficient Grout. In Proceedings of the CORROSION 2013, Orlando, FL, USA, 17–21 March 2013; NACE International: Houston, TX, USA, 2013.
13. Lau, K.; Lasa, I.; Paredes, M. Bridge tendon failures in the presence of deficient grout. *Mater. Perform.* **2013**, *52*, 64–68.
14. Lau, K.; Lasa, I.; Paredes, M. Update on Corrosion of Post-Tensioned Tendons with Deficient Grout. In Proceedings of the CORROSION 2014, San Antonio, TX, USA, 9–13 March 2014; NACE International: Houston, TX, USA, 2014.
15. Lee, S.K.; Zielske, J. *An FHWA Special Study: Post-Tensioning Tendon Grout Chloride Thresholds*; FHWA-HRT-14-039; U.S. Department of Transportation, Federal Highway Administration: McLean, VA, USA, May 2014.
16. Theyo, T.; Hartt, W.H.; Paczkowski, P. *Guidelines for Sampling, Assessing, and Restoring Defective Grout in Prestressed Concrete Bridge Post-Tensioning Ducts*; FHWA-HRT-13-028; FHWA-HRT-14-039; U.S. Department of Transportation, Federal Highway Administration: McLean, VA, USA, October 2013.
17. Lee, S.K. *Corrosivity of Water-Soluble Sulfate Ions in Simulated Pore Water Solutions and Different Types of Grout Samples*; No. FHWA-HRT-21-052; Federal Highway Administration. Office of Infrastructure Research and Development: McLean, VA, USA, 2021.
18. Permeh, S.; Krishna Vigneshwaran, K.K.; Lau, K.; Lasa, I. Corrosion of PT Tendons in Deficient Grout in Presence of Enhanced Sulfate and Chloride Concentration. In Proceedings of the NACE Corrosion Risk Management Conference, Houston, TX, USA, 23–25 May 2016; Paper No. 16-18751. NACE: Houston, TX, USA, 2016.
19. Permeh, S.; Krishna Vigneshwaran, K.K.; Lau, K.; Lasa, I. Corrosion of Post-Tensioned Tendons with Deficient Grout, Part 3: Segregated Grout with Elevated Sulfate and Vestigial Chloride Content. *Corrosion* **2019**, *75*, 848–864. [[CrossRef](#)]
20. Sonawane, R.; Permeh, S.; Lau, K.; Duncan, M.; Simmons, R. Review on the Determination of Sulfate Ion Concentrations in Deficient Post-Tensioned Grouts. In Proceedings of the CORROSION 2021, Virtual Conference, 19–30 April 2021; NACE International: Houston, TX, USA, 2021.
21. Sonawane, R.; Permeh, S.; Lau, K. Development of deficient grout and corrosion due to water and solute transport. In Proceedings of the 1st Corrosion and Materials Degradation Web Conference, Virtual Conference, 17–19 May 2021; MDPI: Basel, Switzerland, 2021. [[CrossRef](#)]
22. Permeh, S.; Lau, K.; Tansel, B. Moisture and ion mobilization and stratification in post-tensioned (PT) grout during hydration. *Case Stud. Constr. Mater.* **2021**, *15*, e00644. [[CrossRef](#)]
23. Permeh, S.; Lau, K. *Accelerated Corrosion Testing of Grouts for PT Steel Strand*; Final Report to Florida Department of Transportation, Contract No. BDV29-977-44; Florida Department of Transportation: Tallahassee, FL, USA, April 2021.
24. Alexander, C.L.; Chen, Y.M.; Orazem, M.E. *Impedance-Based Detection of Corrosion in Post-Tensioned Cables: Phase 2 from Concept to Application*; Final Report to Florida Department of Transportation, Contract No. BDV31-977-35; Florida Department of Transportation: Tallahassee, FL, USA, July 2017.
25. Alexander, C.L.; Orazem, M.E. Indirect electrochemical impedance spectroscopy for corrosion detection in external post-tensioned tendons: 1. Proof of concept. *Corros. Sci.* **2020**, *164*, 108331. [[CrossRef](#)]
26. Taveira, L.V.; Joseph, B.; Sagüés, A.A.; Sabando, J.L. Detection of corrosion of post-tensioned strands in grouted assemblies. In Proceedings of the CORROSION 2008, New Orleans, LA, USA, 16 March 2008; NACE International: Houston, TX, USA, 2008.
27. Azizinamini, A.; Gull, J. *Improved Inspection Techniques for Steel Prestressing/Post-Tensioning Strand: Volume I*; Contract No. BDV80-977-13; Final Report to Florida Department of Transportation; FDOT Research Center: Tallahassee, FL, USA, June 2012.
28. Dukeman, D.; Freij, H.; Sagüés, A.A.; Alexander, C. *Field Demonstration of Tendon Imaging Methods*; Contract No. BDV25-977-52; Final Report to Florida Department of Transportation; FDOT Research Center: Tallahassee, FL, USA, July 2019.
29. Hartt, W.H.; Lee, S.K. Modeling and projecting the onset and subsequent failure rate of corroding bridge post-tension tendons arising from deficient grout. *Corrosion* **2018**, *74*, 241–248. [[CrossRef](#)]
30. Hartt, W.H. Effect of Modeling Variables upon Projection of Corrosion-Induced Bridge Post-Tension Tendon Failures. *Corrosion* **2019**, *74*, 768–775. [[CrossRef](#)]

31. Whitmore, D.; Lasa, I. Impregnation technique provides corrosion protection to grouted post-tensioning tendons. *MATEC Web Conf.* **2018**, *199*, 05008. [[CrossRef](#)]
32. Whitmore, D.; Lasa, I. Cable Impregnation for Post-Tension Grouting Problems. In *Transportation 2014: Past, Present, Future-2014 Conference and Exhibition of the Transportation Association of Canada//Transport 2014: Du passé vers l'avenir-2014 Congrès et Exposition de l'Association des transports du Canada*; Transportation Association of Canada: Ottawa, ON, Canada, 2014.
33. Hamilton, H.R.; Piper, A.; Randell, A.; Brunner, B. *Simulation of Prepackaged Grout Bleed under Field Conditions*; Final Report to Florida Department of Transportation; BDK75-977-59; Department of Civil and Coastal Engineering, University of Florida: Tallahassee, FL, USA, April 2014.
34. Hamilton, H.R.; Torres, E.; Aguirre, M.; Ferraro, C.C. *Evaluation of Shelf Life in Post-Tensioning Grouts*; BDV31-977-31; Final Report to Florida Department of Transportation; Department of Civil and Coastal Engineering, University of Florida: Tallahassee, FL, USA, November 2018.
35. Hamilton, H.R. *Evaluation of Techniques to Remove Defective Grout from Post-Tensioning Tendons*; BDV31-977-58; Final Report to Florida Department of Transportation; University of Florida: Gainesville, FL, USA, February 2020.
36. Whitmore, D.; Tore Arnesen, P.E. Evaluation and Mitigation of Post-Tensioned Steel Corrosion. In Proceedings of the Eighth Congress on Forensic Engineering, ASCE, Reston, VA, USA, 29 November–2 December 2018.
37. Rehm, S.; Lau, K.; Azizinamini, A. *Development of Quality Assurance and Quality Control System for Post Tensioned Segmental Bridges in Florida: Case of Ringling Bridge—Phase II*; BDV29-977-34; Final Report to Florida Department of Transportation; FDOT Research Center: Tallahassee, FL, USA, March 2019.
38. Hurlbaeus, S.; Hueste, M.; Karthik, M.; Terzioglu, T. *Condition Assessment of Bridge Post-Tensioning and Stay Cable Systems Using NDE Methods*; Final Report to National Cooperative Highway Research Program (NCHRP), Project No. 14–28; Transportation Research Board of the National Academies: Washington, DC, USA, September 2016.
39. Permeh, S.; Lau, K.; Duncan, M.; Simmons, R. Identification of steel corrosion in alkaline sulfate solution by electrochemical noise. *Mater. Corros.* **2021**, *72*, 1456–1467. [[CrossRef](#)]
40. Jones, D. *Principles and Prevention of Corrosion*, 2nd ed.; Prentice Hall: Upper Saddle River, NJ, USA, 1996.
41. Bentur, A.; Diamond, S.; Berke, N.S. *Steel Corrosion in Concrete: Fundamentals and Civil Engineering Practice*, 1st ed.; CRC Press: Boca Raton, FL, USA, 1997. [[CrossRef](#)]
42. Bertolini, L.; Elsener, B.; Pedferri, P.; Redaelli, E.; Polder, R.B. *Corrosion of Steel in Concrete: Prevention, Diagnosis, Repair*; John Wiley & Sons: Hoboken, NJ, USA, 2013.
43. *ASTM C876-(2015)*; Standard Test Method for Corrosion Potentials of Uncoated Reinforcing Steel in Concrete. ASTM: West Conshohocken, PA, USA, 2015.
44. Krishna Vigneshwaran, K.K.; Permeh, S.; Lasa, I.; Lau, K. Corrosion of Steel in Deficient Grout with Enhanced Sulfate Content. In Proceedings of the NACE Concrete Service Life Extension Conference, Philadelphia, PA, USA, 1 July 2015; Paper No. CCC15-6942. NACE: Houston, TX, USA, 2015.
45. Permeh, S.; Krishna Vigneshwaran, K.K.; Lau, K.; Lasa, I.; Paredes, M. Material and Corrosion Evaluation of Deficient PT Grout with Enhanced Sulfate Concentrations. In Proceedings of the CORROSION 2015, Dallas, TX, USA, 15–19 March 2015; NACE International: Houston, TX, USA, 2015.
46. Permeh, S.; Krishna Vigneshwaran, K.K.; Echeverría, M.; Lau, K.; Lasa, I. Corrosion of Post-Tensioned Tendons with Deficient Grout, Part 2: Segregated Grout with Elevated Sulfate Content. *Corrosion* **2018**, *74*, 457–467 2018. [[CrossRef](#)]
47. Feliu, S.; González, J.; Andrade, M.C.; Feliu, V. Determining polarization resistance in reinforced concrete slabs. *Corros. Sci.* **1989**, *29*, 105–113. [[CrossRef](#)]
48. Feliu, S.; Galvan, J.C.; Feliu, S., Jr.; Simancas, J.; Bastidas, J.M.; Morcillo, M.; Almeida, E. Differences between apparent polarization resistance values obtained in the time and frequency domains. *J. Electroanal. Chem.* **1995**, *381*, 1–4. [[CrossRef](#)]
49. Krishna Vigneshwaran, K.K.; Permeh, S.; Echeverría, M.; Lau, K.; Lasa, I. Corrosion of Post-Tensioned Tendons with Deficient Grout, Part 1: Electrochemical Behavior of Steel in Alkaline Sulfate Solutions. *Corrosion* **2018**, *74*, 362–371. [[CrossRef](#)]
50. Wang, H.; Sagüés, A.A.; Powers, R.G. Corrosion of the strand-anchorage system in post-tensioned grouted assemblies. In Proceedings of the CORROSION 2005, Houston, TX, USA, April 2005; NACE International: Houston, TX, USA, 2005.
51. Darwin, D.; Sturgeon, W. *Rapid Macrocell Tests of Enduramet Steel Bars*; The University of Kansas Center for Research, Inc.: Lawrence, KS, USA, January 2011.
52. O'Reilly, M.; Darwin, D.; Browning, J. *Corrosion Performance of Prestressing Strands in Contact with Dissimilar Grouts*; No. KS-12-4; Department of Transportation: Washington, DC, USA, 2013.
53. O'Reilly, M.; Darwin, D.; Browning, J. Corrosion Performance of Prestressing Strands in Contact with Dissimilar Grouts. *ACI Mater. J.* **2015**, *112*, 491–500. [[CrossRef](#)]
54. Rafols, J.C.; Lau, K.; Lasa, I.; Paredes, M.; ElSafty, A. Approach to determine corrosion propensity in post-tensioned tendons with deficient grout. *Open J. Civ. Eng.* **2013**, *3*, 36394. [[CrossRef](#)]
55. Sonawane, R.; Permeh, S.; Garber, D.; Lau, K.; Simmons, R.; Duncan, M. Test Methods to Identify Robustness of Grout Materials to Resist Corrosion. In Proceedings of the CORROSION 2020, Digital Proceedings, Lviv, Ukraine, 14–18 June 2020; NACE International: Houston, TX, USA, 2020.

56. Permeh, S.; Sonawane, R.; Lau, K.; Duncan, M.; Simmons, R. Update on the Evaluation of Grout Robustness and Corrosion by Accelerated Corrosion and Rapid Macrocell Testing. In Proceedings of the CORROSION 2021, Virtual Conference, 19–30 April 2021; NACE International: Houston, TX, USA, 2021.
57. Permeh, S.; Lau, K.; Tansel, B. *Development of Standard Methodology to Measure Sulfate Ions in Post-Tensioned Grouts*; Final Report to Florida Department of Transportation, Contract No. BDV29-977-43; Florida Department of Transportation: Tallahassee, FL, USA, April 2021.
58. Permeh, S.; Lau, K.; Matthew, D. Accelerated Testing to Assess Robustness of Post-Tensioning Grout. *Mater. Perform.* **2021**, *60*, 34–38.
59. Bertolini, L.; Carsana, M. High pH corrosion of prestressing steel in segregated grout. *Model. Corroding Concr. Struct.* **2011**, *5*, 147–158.
60. Carsana, M.; Bertolini, L. Characterization of segregated grout promoting corrosion of posttensioning tendons. *J. Mater. Civ. Eng.* **2016**, *28*, 04016009. [[CrossRef](#)]
61. Krishna Vigneshwaran, K.K.; Lau, K.; Permeh, S.; Lasa, I. Anodic Behavior of Steel in Enhanced Sulfate Solutions. In Proceedings of the CORROSION 2016, Vancouver, BC, Canada, 6–10 March 2016; NACE International: Houston, TX, USA, 2016.
62. Echeverria, M.; Lau, K.; Permeh, S. Anodic Behavior of Steel in Sulfate-Rich Simulated Grout Pore Solution. In *ECS Meeting Abstracts*; IOP Publishing: Bristol, UK, September 2017; p. 801. [[CrossRef](#)]
63. Kelly, R.G.; Scully, J.R.; Shoemith, D.; Buchheit, R.G. *Electrochemical Techniques in Corrosion Science and Engineering*; CRC Press: Boca Raton, FL, USA, 2002.
64. Orazem, M.E.; Tribollet, B. *Electrochemical Impedance Spectroscopy*; John Wiley & Sons, Inc.: Hoboken, NJ, USA, 2008.
65. Lau, K.; Paredes, M.; Rafols, J. Corrosion Evaluation of Post-Tensioned Tendons with Dissimilar Grout. In Proceedings of the CORROSION 2012, Salt Lake City, UT, USA, 11–15 March 2012; NACE International: Houston, TX, USA, 2015.
66. Permeh, S.; Lau, K.; Duncan, M.; Simmons, R. Initiation of localized steel corrosion in alkaline sulfate solution. *Mater. Struct.* **2021**, *54*, 143. [[CrossRef](#)]
67. Permeh, S.; Lau, K. Corrosion of post-tension tendons associated with segregated grout. In Proceedings of the 1st Corrosion and Materials Degradation Web Conference, Virtual Conference, 17–19 May 2021; MDPI: Basel, Switzerland, 2021. [[CrossRef](#)]
68. Ritter, S.; Huet, F.; Cottis, R.A. Guideline for an assessment of electrochemical noise measurement devices. *Mater. Corros.* **2012**, *63*, 297–302. [[CrossRef](#)]
69. Cottis, R. Interpretation of Electrochemical Noise Data. *Corrosion* **2001**, *57*, 265–285. [[CrossRef](#)]